

Discovery of natural berberine-derived nitroimidazoles as potentially multi-targeting agents against drug-resistant *Escherichia coli*

Guo-Biao Zhang, Swetha Kameswari Maddili, Vijai Kumar Reddy Tangadanchu, Lavanya Gopala, Wei-Wei Gao, Gui-Xin Cai* & Cheng-He Zhou*

Institute of Bioorganic & Medicinal Chemistry, Key Laboratory of Applied Chemistry of Chongqing Municipality, School of Chemistry and Chemical Engineering, Southwest University, Chongqing 400715, China

Received September 26, 2017; accepted November 1, 2017; published online December 28, 2017

A series of natural berberine-derived nitroimidazoles as novel antibacterial agents were designed, synthesized and characterized by nuclear magnetic resonance (NMR), infrared spectra (IR), and high resolution mass spectra (HRMS) spectra. The antimicrobial evaluation showed that some target molecules exhibited moderate to good inhibitory activities against the tested bacteria and fungi including clinical drug-resistant strains isolated from infected patients. Especially, 2-fluorobenzyl derivative **8f** not only gave strong activity against drug-resistant *E. coli* with the minimal inhibitory concentration (MIC) value of 0.003 mM, 33-fold more active than norfloxacin, but also exhibited low toxicity toward RAW 264.7 cells and less propensity to trigger resistance. The aqueous solubility and *ClogP* values of target compounds were investigated to elucidate the structure-activity relationships. Molecular docking and quantum chemical studies for compound **8f** rationally explained its antibacterial effect. The further exploration of antibacterial mechanism revealed that the highly active compound **8f** could effectively permeabilize *E. coli* cell membrane and intercalate into DNA isolated from resistant *E. coli* to form **8f**-DNA complex that might block DNA replication to exert the powerful bioactivities. Compound **8f** could also selectively address resistant *E. coli* from a mixture of various strains.

berberine, nitroimidazole, *Escherichia coli*, DNA, membrane permeabilization

Citation: Zhang GB, Maddili SK, Tangadanchu VKR, Gopala L, Gao WW, Cai GX, Zhou CH. Discovery of natural berberine-derived nitroimidazoles as potentially multi-targeting agents against drug-resistant *Escherichia coli*. *Sci China Chem*, 2018, 61: 557–568, <https://doi.org/10.1007/s11426-017-9169-4>

1 Introduction

The emergence of antibiotics brought a vital revolution toward previously fatal microbial infections, and the discovery of antibacterial sulfonamides and penicillins further spurred the development of additional classes of antimicrobial agents, which successfully kept infectious diseases in control [1]. However, the misuse and inappropriate use of various antibiotics have created unprecedented conditions for mo-

bilizing resistance elements in microbial populations, which directly led to the emergence and spread of resistant strains like methicillin-resistant *Staphylococcus aureus* (MRSA), vancomycin-resistant *Enterococcus faecium* (VRE), and fluoroquinolone-resistant *Escherichia coli* (*E. coli*) [2]. Seriously, *E. coli* has been extensively found to have the recently emerged and globally disseminated resistance to various clinical antibacterial drugs such as fluoroquinolones, aminoglycosides, trimethoprim-sulfamethoxazoles, and carbapenems due to the overexpression of multidrug efflux pumps and the enhanced function of cell membrane. The

*Corresponding authors (email: gxcai@swu.edu.cn; zhouch@swu.edu.cn)

drug-resistant *E. coli* as an increasing menace could lead to urinary tract infection, cause injury of ureter contractility and form intracellular bacterial communities in the bladder [3]. Therefore, the World Health Organization initiated a global action plan calling on all countries to adopt measures against drug-resistant microbes, and the discovery of new antimicrobial drugs with novel mechanisms has been an urgent need to combat resistant strains.

The antimicrobial drug discovery is quite difficult probably due to the poor permeation of compounds across the microbial cell membrane [4]. Some natural products, which can break through the penetration barriers, are historically significant as lead compounds for antimicrobials [5]. The natural berberine, occurring as a mainly pharmacological component in various plants including *Rhizoma coptidis*, *Phellodendron amurense* and *Barberry*, has long been utilized as Chinese traditional medicine for the treatment of diarrhea since 2000 years ago [6]. The good antibacterial efficiency of berberine might be on account of its large π -conjugated backbone binding to both single- and double-stranded DNA in microorganisms through π - π stacking and electronic interactions [7]. The long-historical use of berberine has not obviously triggered the development of drug-resistance till today, which showed that the bacteria still cannot identify and respond to its antibacterial mechanisms. However, the poor solubility and bioavailability of berberine, which was probably attributed to the rigidly planar structure, greatly limited its clinical use [8]. Some researches suggested that the break of planar structure should be favorable for improving solubility and antibacterial activities [9].

Nitroimidazole is an important moiety widely presented in clinical drugs, such as dimetridazole, metronidazole, nimorazole and tinidazole, with broad spectrum activity against bacteria and parasites [10], and its unique aromatic five-membered heterocycle is favorable to effectively interact with biologically important species such as DNAs, enzymes and receptors [11]. It is generally considered that the nitro group will be reduced to reactive radical species, which can directly react with cellular components to inhibit the growth of bacteria [12]. However, resistance has occurred due to the decreased expression and activity of reductive enzymes in target cell. A lot of work revealed that the modification of nitroimidazole by large structural fragments might sterically stabilize nitro group to strengthen the interaction with reductive enzymes and enhance the metabolism [13]. Furthermore, the introduction of nitroimidazole, which might be beneficial for the improvement of solubility and bioavailability, has been an important and prevalent strategy to modify natural products to be the potential clinical drugs.

In view of this situation and the important function of heterocyclic azoles [14] by the use of non-covalent bonds in exerting biological activity, as a further extension of our

previous work that the introduction of triazole [15], imidazole [16] and benzimidazole [17] to berberine backbone could result in highly bioactive molecules, a series of hybrids of berberine and nitroimidazole via an ethylenic bond bridge were designed and synthesized for the first time. The design of target compounds was mainly from following three aspects: (1) reduction of aromatic ring of berberine to convert the planar structure into the bended skeleton was expected to increase molecular flexibility and solubility; (2) the ethylenic bond-bridged new π -conjugated skeleton was constructed to compensate the reduced aromatic ring and maintain the DNA binding affinity of target molecules; (3) various aliphatic substituents and benzyl moieties as regulators to ameliorate physicochemical properties were introduced to investigate their effects on antimicrobial activities. It was expected that these novel hybrids of two different antibacterial fragments could not only increase solubility and bioavailability but also strengthen DNA binding affinity and membrane permeabilization, thus exhibiting good potency against bacteria, especially the drug-resistant strains. The natural berberine was used as starting material to construct berberine-derived nitroimidazoles. The target molecules were confirmed by spectral analysis, screened for the antibacterial and antifungal activities *in vitro*, and investigated for the aqueous solubility and Clog P values in order to elucidate the structure-activity relationships. The cell toxicity and antibacterial resistance were further evaluated for the highly active compound. Molecular docking and quantum chemical studies were employed to rationally explain the potent antibacterial effect of the most active molecule. Additionally, the cell membrane permeabilization and binding behavior to DNA, isolated from sensitive bacteria, toward the highly active compound were studied to further explore the possible antibacterial mechanism.

2 Experimental

2.1 Materials and measurement

Melting points of the synthesized compounds were measured by the use of X-6 melting point apparatus (Beijing Focus Instrument CO., Ltd., China) and were uncorrected. Thin layer chromatography (TLC) analysis was performed through pre-coated silica gel plates. Bruker RFS100/S spectrophotometer (Bio-Rad, USA) was employed to record Fourier transform infrared spectra (FT-IR) using potassium bromide pellets in the 4000–400 cm^{-1} range. Nuclear magnetic resonance (NMR) spectra were carried out using Bruker AV 600 spectrometer (Germany) and tetramethylsilane (TMS) as an internal standard. The chemical shifts were recorded with the unit of parts per million (ppm), the signals were described as singlet (s), doublet (d), triplet (t) as well as multiplet (m) and coupling constants (J) were expressed in

hertz (Hz). The following abbreviations were used to designate fragments: Ber=berberine, Im=nitroimidazole, Ph=phenyl. The high resolution mass spectra (HRMS) were achieved by IonSpec FTICR mass spectrometer (Waters Micromass, USA) using ESI resource. All fluorescence spectra were recorded on F-7000 spectrofluorimeter (Hitachi, Japan) and UV spectra were obtained through TU-2450 spectrophotometer (Puxi Analytic Instrument Ltd. of Beijing, China), both of which were equipped with 1.0 cm quartz cells. The microbial strains were obtained from Sichuan Provincial People's Hospital (Chengdu, China) and neutral red (NR) was obtained from Sigma-Aldrich (USA). The RAW 264.7 cells were obtained from Kunming wildlife cell bank of the Chinese Academy of Sciences, Kunming, China. Tris(hydroxymethyl)methylamine, sodium chloride and hydrochloric acid were analytical purity. The masses of samples were weighed using microbalance with a resolution of 0.1 mg. All other chemicals and solvents were commercially available and directly used without further purification.

2.2 Synthesis

The detailed synthetic procedures and spectral data for compounds **6–8** were available in the Supporting Information online.

2.3 Antibacterial assay

The berberine-derived nitroimidazoles **6–8** were evaluated for their antibacterial activities against six Gram-positive bacteria (Methicillin-Resistant *Staphylococcus aureus* N315, *Enterococcus faecalis*, *Staphylococcus aureus*, *Staphylococcus aureus* ATCC25923, *Bacillus subtilis* ATCC6633, *Micrococcus luteus* ATCC4698) and six Gram-negative bacteria (*Klebsiella pneumoniae*, *Escherichia coli*, *Escherichia coli* ATCC25922, *Pseudomonas aeruginosa*, *Pseudomonas aeruginosa* ATCC27853, *Acinetobacter baumannii*) including drug-resistant strains (without ATCC number) isolated from infected patients. The bacterial suspension was adjusted with sterile saline to a concentration of 1×10^5 CFU measured by nephelometer. Initially the compounds were dissolved in dimethyl sulfoxide (DMSO) to prepare the stock solutions, then the tested compounds and reference drugs were prepared in Mueller-Hinton broth (Guangdong Huaikai Microbial Sci. & Tech Co., Ltd, Guangzhou, China) to obtain the required concentrations. These dilutions were inoculated and incubated at 37 °C for 24 h.

2.4 Cytotoxicity assay

The stock solutions of compound **8f** and berberine (1024 µg/mL, in DMSO) were prepared in medium and se-

rially diluted. RAW 264.7 cells were grown as monolayer in medium (90% DMEM medium, 10% fetal bovine serum, 1% penicillin/streptomycin) and maintained at 37 °C in a humidified atmosphere containing 5% CO₂. Cells were detached from culture flasks with 0.25% trypsin and 0.03% ethylene diamine tetraacetic acid (EDTA) and resuspended in fresh culture medium at a density of 1.5×10^5 cells/mL. By using a Falcon 96-well, flat-bottom plate, 100 µL of the cell suspension was added to each of the wells and the cells were incubated for 24 h. The tested cells were treated with compound **8f** and berberine in triplicate at concentrations of 8, 16, 32, 64, 128, 256, and 512 µg/mL, respectively. After incubation with compounds for 72 h, 50 µL of a 2.5 mg/mL solution of 3-(4,5-dimethyl-2-thiazolyl)-2,5-diphenyl-2-*H*-tetrazolium bromide (MTT) in phosphate-buffered saline (PBS) was added to each well and further incubated for 3–4 h. The supernatant was removed, and the cells were dissolved in 150 µL of DMSO. Absorbance values were measured at 490 nm by microplate reader.

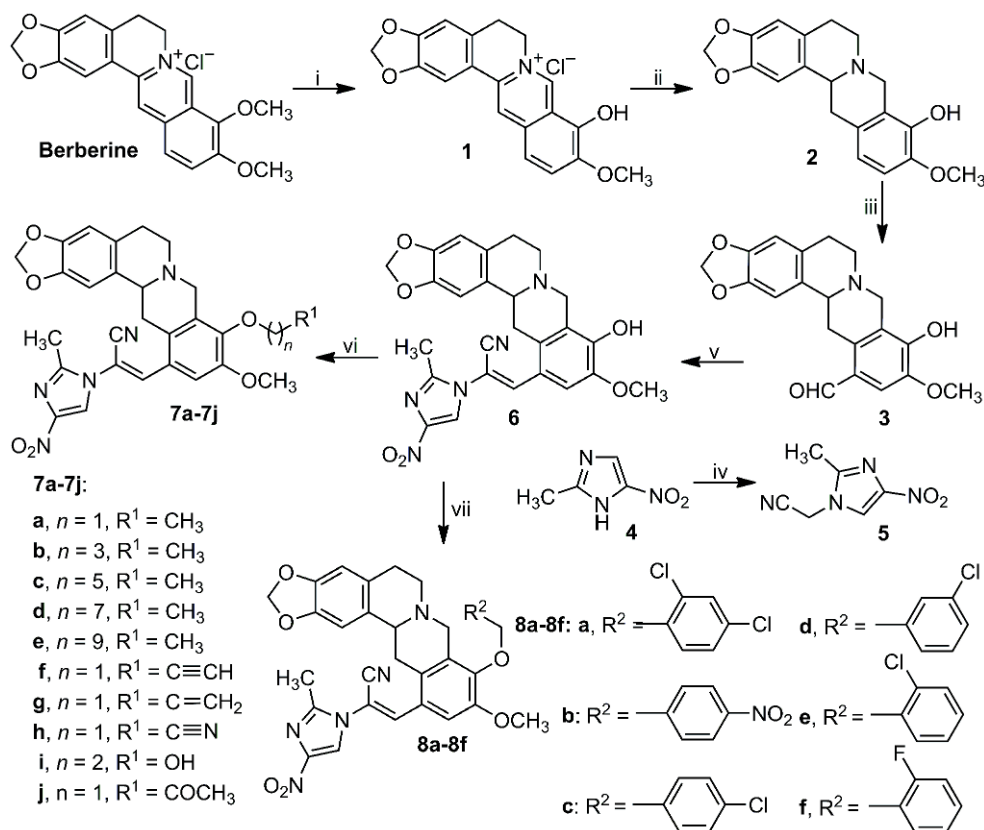
2.5 Resistance study

The representative compound **8f** was selected to investigate the developing rate of bacterial resistance according to the reported method. We exposed a standard strain of resistant *E. coli* toward increasing concentrations of compound **8f** from sub-MIC (0.5×MIC, MIC is the minimal inhibitory concentration) for sustained passages and determined the new MIC values of compound **8f** for each passage of *E. coli*. The initial MIC value of compound **8f** and norfloxacin was determined against *E. coli* as mentioned above in antibacterial assay. For the next MIC experiment, the bacterial dilution was prepared by using the bacteria from sub-MIC concentration of the compound (0.5×MIC). After a 12 h incubation period, again bacterial dilution was prepared by using the bacterial suspension from sub-MIC concentration of the compound (0.5×MIC) and assayed for the next MIC experiment. The process was repeated for 15 passages. The MIC values for compound **8f** against each passage of *E. coli* were determined.

3 Results and discussion

3.1 Chemistry

The berberine-derived nitroimidazoles **6–8** were synthesized via multi-step reactions from natural berberine as outlined in Scheme 1. Initially, berberrubine **1** was easily obtained through selective demethylation of commercial berberine in high yield of 89.8%, and the latter was further reduced by excessive sodium borohydride to generate structurally benzened derivative **2** with the yield of 57.0%. Compound **2** was further formylated by hexamethylenetetramine (HMTA)



Scheme 1 The synthesis of berberine-derived nitroimidazoles **6–8**. Reagents and conditions: (i) 190 °C/vacuum, 45 min; (ii) methanol, NaBH₄, 25 °C, 4 h; (iii) (a) HMTA, TFA, 120 °C, 6 h; (b) 10% H₂SO₄, 25 °C, 2 h; (iv) K₂CO₃, chloroacetonitrile, CH₃CN, 80 °C, 2 h; (v) cyanoethyl nitroimidazole **5**, piperidine, CH₃CN, refluxed, 12 h; (vi) aliphatic halides, K₂CO₃, CH₃CN, 80 °C, 12 h; (vii) substituted benzyl halides, K₂CO₃, CH₃CN, 80 °C, 6 h.

using trifluoroacetic acid (TFA) as solvent to conveniently and efficiently produce the corresponding aldehyde **3** with moderate yield of 78.5%. The condensation of intermediate **3** and cyanoethyl nitroimidazole **5**, which was readily prepared from 2-methyl-5-nitroimidazole, could afford compound **6** in the presence of piperidine, and the further *O*-alkylation of hydroxyl compound **6** with various aliphatic and aromatic halides was performed to achieve target compounds **7** and **8** in 12.8%–49.5%. All the new compounds were confirmed by NMR, IR and HRMS spectra. Furthermore, the purity of target molecules was evaluated through quantitative nuclear magnetic resonance (QNMR) method using 1,3,5-trioxane as internal standard, which demonstrated that all the target compounds exerted a purity of at least 95%.

3.2 Spectral analysis

In IR spectra, all the newly synthesized molecules **6–8** gave two broad absorption in 3167–3126 cm⁻¹ and 1662–1619 cm⁻¹ that suggested the presence of ethylenic group. The characteristic C≡N bands in all berberine-derived nitroimidazoles appeared in the region of 2218–2210 cm⁻¹. The strong absorption between 1486–1483 cm⁻¹ indicated the presence of nitro group. All the other absorption bands

were observed at the expected regions. In ¹H NMR spectra, compound **6** gave singlet at 3.99 ppm assigned to *O*-CH₃ protons on berberine backbone. The *O*-alkylation of molecule **6** by alkyl chains to yield berberine derivatives **7a–7e** resulted in little upfield shifts of *O*-CH₃ protons (3.94–3.87 ppm), while the replacement of alkyl chain by aralkyl moiety (**8a–8f**) would lead to little downfield shifts (3.98–3.91 ppm). The chemical shifts of CH₃ protons attached in nitroimidazole ring were lower (2.58–2.55 ppm) than that of *O*-CH₃, which might be attributed to the electron-withdrawing oxygen atom. The peaks for C=CH proton in the target molecules **6–8** appeared at 7.69–7.64 ppm, which were higher than normal alkene protons because of the new large π -conjugated skeleton. All the other protons were observed at the appropriate chemical shifts with expected integral values. In ¹³C NMR spectra, berberine-derived nitroimidazoles **6–8** gave expected signals at 13.8–13.7 ppm which should be assigned to the methyl carbon linked to nitroimidazole ring, while the chemical shifts of *O*-CH₃ carbon in berberine skeleton were higher (56.5–56.0 ppm) due to the presence of oxygen atom. No large difference was found in the ¹³C NMR chemical shifts for 2- and 3- C in the berberine backbone (146.4–146.2 ppm). The signals for 5- C in nitroimidazole ring appeared at 147.6–147.2 ppm, which

indicated little upfield shifts in comparison with normal aromatic carbons because of the presence of electron-withdrawing nitro group. All other carbons ideally gave the signals at the expected regions.

3.3 Analysis of X-ray diffraction

The deprotonation of nitroimidazole **4** by potassium carbonate would produce a tautomeric equilibrium of **A** and **B** isomers in theory (Scheme 2), and subsequently reacted with chloroacetonitrile could generate cyanoethyl nitroimidazoles **5a** and **5b**. In order to understand the structures of the resulting isomer products **5a** or **5b**, give rational explanation for these two isomers and further figure out the absolute configuration of target compounds, the single crystal of cyanoethyl-modified derivative **7h** was cultivated and X-ray diffraction analysis showed that the berberine backbone was combined with nitroimidazole through the 3-*N* position in imidazole nucleus instead of the 1-*N* position, which indicated that it should be isomer **5b** as the main product. Moreover, it was confirmed that the *Z* configuration and *s-trans* conformation were adopted on account of the large steric hindrance of nitroimidazole moiety in berberine-derived nitroimidazole compound **7h** (Figure 1).

3.4 Antimicrobial activity

Table 1 showed that some berberine-derived nitroimidazoles displayed more potent efficacy in comparison with norfloxacin and berberine against the tested bacteria, which suggested that the introduction of nitroimidazole to berberine backbone could greatly optimize the antibacterial activities. The 9-hydroxyl derivative **6** exhibited much better inhibitory effect against resistant bacterial strains *E. coli* and *P. aeruginosa* with lower MIC value of 0.032 mM than berberine (MIC=0.688 mM). Subsequently, the *O*-alkylation of active precursor **6** by hexyl bromide led to the hexyl hybrid **7c** with strong efficiency against *E. faecalis* (MIC=0.027 mM), which was 32-fold and 13-fold more potent than norfloxacin and berberine, respectively. In contrast with **7c**, none of the

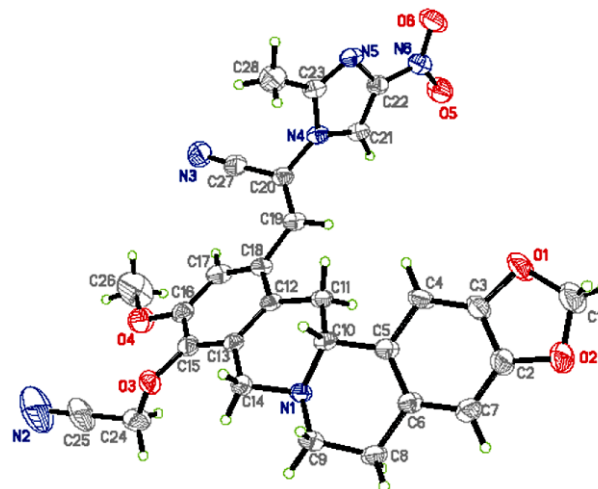
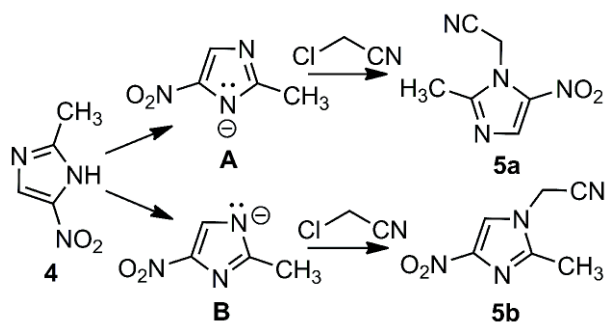


Figure 1 X-ray structure of berberine-derived nitroimidazole compound **7h** (color online).

tested bacteria was sensitive to compound **7a** with short ethyl chain. When the length of alkyl chain increased, the decyl derivative **7e** could effectively suppress the growth of *P. aeruginosa* ATCC27853 with MIC value of 0.012 mM, which was much lower than that of reference drug norfloxacin (MIC=0.100 mM), while the short unsaturated hydrocarbon modified compounds **7f** and **7g** gave better inhibitory activity against the tested bacteria than short alkyl derivatives **7a** and **7b**. Obviously, the hydroxyl and carbonyl incorporated compounds **7i** and **7j** also exerted profound antibacterial effects with low MIC values toward clinical drug-resistant bacteria. These results dramatically suggested that the long length of aliphatic chain should be favorable for the inhibition of bacteria, which might be attributed to the improved lipophilicity, and the introduction of unsaturated groups could also significantly strengthen antibacterial activity. Furthermore, the hydroxyl and carbonyl groups smoothly gave positive influence on the bioactivity, which might be on account of the formation of hydrogen bonds between compound and biologically important species.

The *in vitro* antifungal screening revealed that some prepared berberine nitroimidazoles exhibited good efficacies on the inhibition of the tested fungal strains. Compound **6** displayed moderate to good activities with MIC values ranging from 0.016 to 1.003 mM. In the series of **7a–7j**, compound **7e** bearing decyl chain generally gave good anti-*C. albicans* activity with MIC value of 0.025 mM. The replacement of decyl group by ethoxyl fragment, which generated compound **7i**, resulted in better efficiency to suppress *C. tropicalis* with MIC value of 0.015 mM, which was 23-fold and 56-fold more potent than reference drugs berberine and fluconazole, respectively. Especially, the 2-fluorobenzyl derivative **8f** showed profound effect against *A. fumigatus* with MIC value of 0.026 mM.



Scheme 2 Possible mechanism for the syntheses of cyanoethyl nitroimidazole **5**.

Table 1 MIC (mM) for berberine-derived nitroimidazoles **6–8** against Gram-positive and Gram-negative bacteria

Compound	Gram-positive bacteria ^{a), b)}						Gram-negative bacteria ^{c)}					
	MRSA	<i>E. faecalis</i>	<i>S. aureus</i>	<i>S. aureus</i> ATCC25923	<i>B. subtilis</i> ATCC6633	<i>M. luteus</i> ATCC4698	<i>K. pneumoniae</i>	<i>E. coli</i>	<i>E. coli</i> ATCC25922	<i>P. aeruginosa</i>	<i>P. aeruginosa</i> ATCC27853	<i>A. baumannii</i>
6	0.255	0.128	0.128	0.032	0.255	1.021	0.064	0.032	0.128	0.032	0.032	0.064
7a	0.967	0.242	0.483	0.967	0.483	0.242	0.483	0.121	0.242	0.121	0.242	0.483
7b	0.459	0.918	0.459	0.459	0.459	0.459	0.230	0.115	0.459	0.918	0.918	0.230
7c	0.437	0.027	0.437	0.437	0.437	0.437	0.109	0.437	0.109	0.874	0.874	0.054
7d	0.209	0.052	0.834	0.209	0.209	0.209	0.209	0.104	0.417	0.834	0.104	0.417
7e	0.100	0.025	0.100	0.100	0.798	0.399	0.399	0.100	0.399	0.100	0.012	0.399
7f	0.119	0.237	0.237	0.119	0.237	0.237	0.474	0.119	0.474	0.119	0.237	0.237
7g	0.473	0.118	0.236	0.473	0.473	0.473	0.473	0.236	0.236	0.473	0.473	0.236
7h	0.118	0.474	0.118	0.118	0.237	0.474	0.118	0.118	0.118	0.947	0.947	0.474
7i	0.117	0.059	0.117	0.117	0.469	0.469	0.938	0.059	0.469	0.235	0.235	0.029
7j	0.029	0.918	0.230	0.029	0.459	0.459	0.115	0.029	0.115	0.115	0.115	0.115
8a	0.049	0.777	0.388	0.024	0.388	0.388	0.388	0.777	0.388	0.777	0.194	0.777
8b	0.201	0.805	0.402	0.201	0.805	0.402	0.805	0.050	0.402	0.805	0.805	0.805
8c	0.818	0.051	0.409	0.818	0.409	0.818	0.102	0.409	0.204	0.818	0.818	0.818
8d	0.409	0.204	0.818	0.409	0.818	0.818	0.818	0.818	0.409	0.818	0.102	0.204
8e	0.409	0.409	0.818	0.409	0.204	0.409	0.409	0.204	0.102	0.409	0.818	0.818
8f	0.013	0.210	0.420	0.013	0.210	0.420	0.052	0.003	0.105	0.420	0.026	0.007
Berberine	0.688	0.344	0.011	0.172	0.344	0.344	0.344	0.688	0.688	0.688	0.344	0.688
Norfloxacin	0.013	0.802	0.200	0.050	0.050	0.013	1.603	0.100	0.003	0.013	0.100	0.025

a) Minimal inhibitory concentrations were determined by micro broth dilution method for microdilution plates; b) MRSA, methicillin-resistant *Staphylococcus aureus* (N315); *E. faecalis*, *Enterococcus faecalis*; *S. aureus*, *Staphylococcus aureus*; *S. aureus* ATCC25923, *Staphylococcus aureus* (ATCC25923); *B. subtilis* ATCC6633, *Bacillus subtilis* ATCC6633; *M. luteus* ATCC4698, *Micrococcus luteus* (ATCC4698); c) *K. pneumoniae*, *Klebsiella pneumoniae*; *E. coli*, *Escherichia coli*; *E. coli* ATCC25922, *Escherichia coli* ATCC25922; *P. aeruginosa*, *Pseudomonas aeruginosa*; *P. aeruginosa* ATCC27853, *Pseudomonas aeruginosa* ATCC27853; *A. baumannii*, *Acinetobacter baumannii*.

3.5 Analysis of ClogP values and aqueous solubility

Lipophilicity/hydrophilicity directly exerts important influence in various biological processes of bioactive molecules including transportation, distribution, metabolism and secretion [20]. Therefore, it is quite necessary to have a good knowledge of lipophilicity/hydrophilicity to predict the bioactivity of drugs. The theoretically calculated values of logP (ClogP) for all the berberine-derived nitroimidazoles were obtained by the use of software ChemDraw Ultra 14.0 (Table 2). Obviously, most of the berberine-derived nitroimidazoles were lipophilic (ClogP=2.34–8.07), which was related to the length of aliphatic chain and the number of halogen atom on benzene ring. The relationship of all the target compounds between ClogP and antibacterial effect against drug-resistant *E. coli* was successfully investigated as shown in Figure 2. In general, the evaluated compounds with high values of ClogP usually showed poor inhibitory activities. The relatively lower lipophilicity/hydrophilicity partition coefficient (ClogP<5.5) remarkably resulted in profound efficiency against *E. coli*, which suggested that the introduction of lipophilic moiety was favorable for the antibacterial activities.

Numerous promising drug candidates commonly suffered

Table 2 ClogP values and evaluation of solubility of berberine-derived nitroimidazoles (mean±SD, n=3) ^{a), b)}

Compound	ClogP	Aqueous solubility	Compound	ClogP	Aqueous solubility
6	2.83	5.04±0.27	7i	2.43	8.13±0.31
7a	3.83	4.79±0.06	7j	2.66	4.14±0.17
7b	4.89	1.65±0.34	8a	6.50	0.11±0.04
7c	5.95	6.49±0.14	8b	4.82	7.09±0.11
7d	7.01	0.21±0.01	8c	5.79	1.65±0.19
7e	8.07	0.09±0.02	8d	5.79	2.01±0.20
7f	3.72	5.31±0.09	8e	5.79	0.13±0.15
7g	4.08	3.34±0.17	8f	5.22	4.54±0.08
7h	2.34	6.71±0.12	Berberine	-0.77	4.08±0.02

a) ClogP values were calculated by ChemDraw Ultra 14.0; b) in µg/mL, determined in pH 7.4 phosphate buffer, at 30 °C.

from poor aqueous solubility, which would lead to incomplete absorption and hinder their application in clinical cases. Thus, aqueous solubility is an important parameter for potential drug [21]. The aqueous solubility of all the target compounds was evaluated at physiological pH to further elucidate the affection of various substituents on solubility and antibacterial activity, and the obtained results were

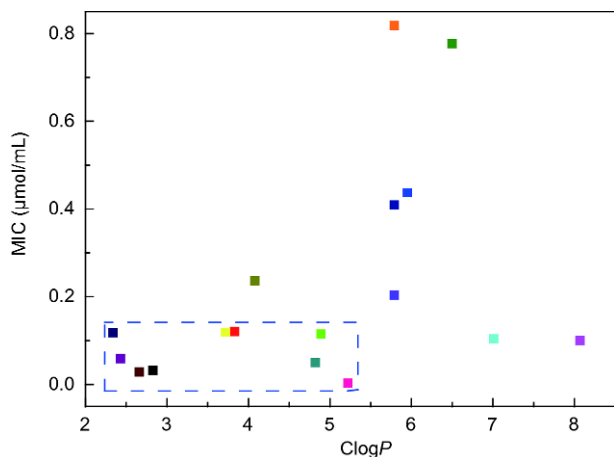


Figure 2 The calculated partition coefficients vs. antibacterial effect against drug-resistant *E. coli*. (color online).

shown in Table 2. Most of the berberine-derived nitroimidazoles gave relatively better water solubility than berberine while some molecules exhibited poor solubility, which might be attributed to the hydrophobic aliphatic chain and benzyl group. For example, compound **7e** with lipophilic decyl chain logically exhibited the lowest aqueous solubility (0.09 $\mu\text{g/mL}$). Furthermore, the contribution of aqueous solubility to the inhibitory potency against resistant *E. coli* was scientifically expressed in Figure 3, which remarkably showed that the highly aqueous solubility (>4 $\mu\text{g/mL}$) could be favorable for the antibacterial activity. In summary, it has demonstrated that the low lipophilicity and high hydrophilicity would be useful for enhancing antibacterial activities.

3.6 Cell toxicity

Assessment of toxicity is a critical component in the drug

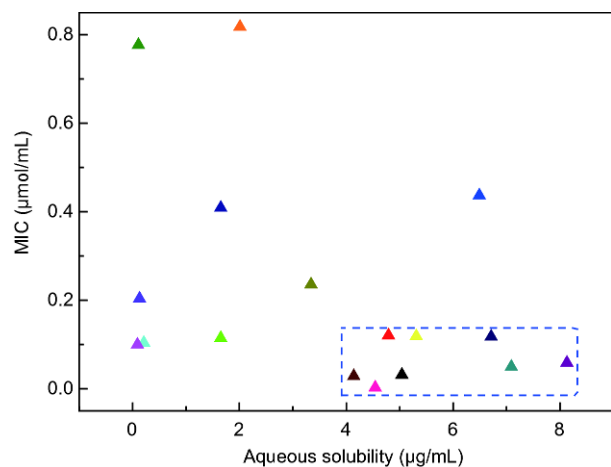


Figure 3 Aqueous solubility vs. antibacterial effect against drug-resistant *E. coli*. (color online).

discovery process [22]. The highly active derivative **8f** was further evaluated for its toxicity toward RAW 264.7 cells by colorimetric cell proliferation MTT assay, and berberine was used as the positive control. The cytotoxic results shown in Figure 4 revealed that the cell viability against 2-fluorobenzyloxy derivative **8f** of RAW 264.7 cells was at least more than 85% within concentration of 16 $\mu\text{g/mL}$ (at this concentration, compound **8f** could effectively inhibit the growth of resistant *E. coli*), which indicated that this molecule exerted good selectivity for *E. coli* over mammalian cells. However, the cell viability was lower against berberine than compound **8f** in all the tested concentrations, which implied that the highly bioactive compound **8f** exhibited lower cell toxicity than its precursor natural berberine.

3.7 Development of resistance

Bacterial resistance is usually defined as natural drug resistance and induced drug resistance. In comparison with natural drug resistance that often results from the lack of target sites for antibiotics, the induced drug resistance can lead to much more severe issue due to the structural and bioactive change of functional biomacromolecules such as DNA, enzymes, efflux pump and cell membrane [23]. Therefore, the evaluation of novel promising drug candidates for inducing bacterial resistance is of great significance [24]. In the present work, most of the berberine-derived nitroimidazoles remarkably exhibited significant effect against clinical drug-resistant bacteria, such as MRSA, *E. faecalis* and *E. coli*. To further evaluate the potency of the highly active compound **8f** toward multidrug-resistant bacteria, the susceptible pathogen *E. coli* was chosen to develop resistance against compound **8f**, and norfloxacin was used as the positive control. The standard strain was exposed to the increasing concentrations of compound **8f** from MIC

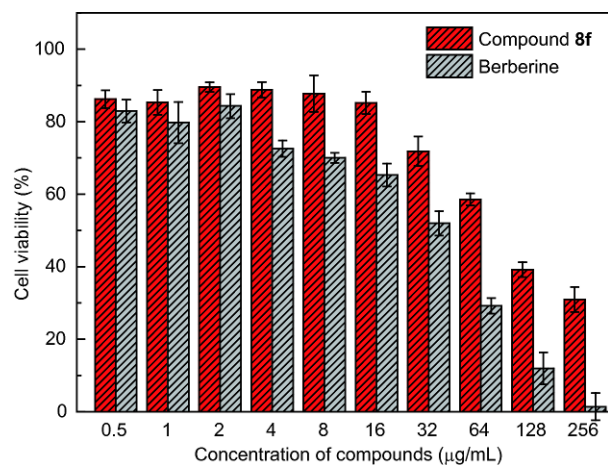


Figure 4 Cytotoxic assay of the active compound **8f** and berberine on RAW 264.7 cells by MTT methodology. Each data bar represents an average of three parallels, and error bar indicates one standard deviation from the mean (color online).

(0.003 mM) for sustained passages and the new MIC values were investigated against each passage of *E. coli*.

As shown in Figure 5, there was no obvious substantial variation in MIC values for compound **8f** during all the 16 passages of *E. coli* strain, whereas norfloxacin significantly gave increasing MIC values after the 9th passage and even around 16-fold increase in MIC was observed after 15th passage. These obtained results showed that clinical drug-resistant *E. coli* was more difficult to develop resistance toward compound **8f** than the clinical drug norfloxacin.

3.8 Electronic properties

The concept of highest occupied molecular orbital (HOMO) and lowest unoccupied molecular orbital (LUMO), which is fundamentally prominent as it gives basic understanding for the chemical stability and reactivity of a given molecule, is recently applied to the rational design of drug molecules [25]. The HOMO can be regarded as the outermost electron containing orbital that tends to give these electrons away as an electron donor, while the LUMO can be considered as the innermost orbital containing free sites to serve as electron receptor [26]. Extending the concept into drug-receptor binding system, the HOMOs of compounds **7c**, **8b** and **8f** were mainly localized on berberine backbone and the LUMOs were primarily focused on the nitroimidazole ring, as shown in Table 3. These results manifested that the electrophilic interaction might occur between positively charged biological targets and berberine backbone, whereas the nitroimidazole ring could bind to the negatively charged residues of receptor. Besides, it was observed that the substituents at 9-position of berberine skeleton did not directly contribute to the HOMO and LUMO, which suggested

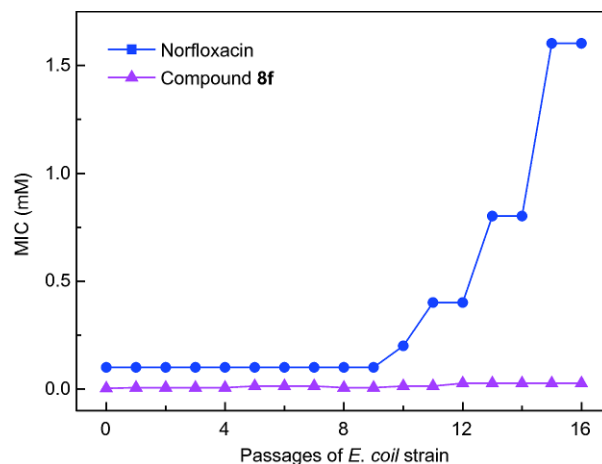


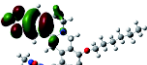
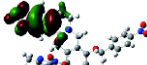
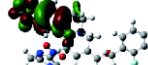
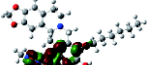
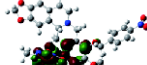
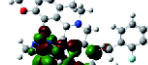
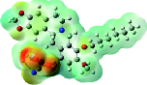
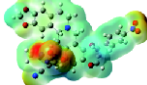
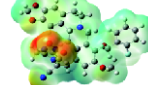
Figure 5 Evaluation of resistance development against compound **8f** in drug-resistant *E. coli*. (color online).

that these groups might be primarily used to regulate the physicochemical characterizations.

The quantum chemical parameters of compounds **7c**, **8b** and **8f** were calculated to predict the possible biological properties (Table 3). It was known that the electronegative molecule can be a good π -electron acceptor, which further evidenced that the natural berberine-derived nitroimidazoles **7c**, **8b** and **8f** with relatively high electronegativity might interact with various biological species through π - π stacking. Moreover, the suitable global hardness and softness theoretically explained the low toxicity.

The molecular electrostatic potential (MEP) surface generally gives an observation of the charged surface area [27], which can convictively probe the hydrophilicity of molecules, electrostatic interaction between compounds and biological targets and the orientation of drug candidates for

Table 3 Atomic orbital HOMO-LUMO composition and quantum chemical parameters of compounds **7c**, **8b** and **8f**^{a)}

Compound	7c	8b	8f
HOMO (eV)	 $E=-5.58$	 $E=-5.70$	 $E=-5.58$
LUMO (eV)	 $E=-2.38$	 $E=-2.58$	 $E=-2.39$
MEPs			
Electronegativity	3.98	4.14	3.99
Global hardness	1.60	1.56	1.59
Global softness	0.62	0.64	0.63

a) The 3D structure of the molecules were built by Sybyl 2.0 and Gauss 09, and were optimized through the B3LYP hybrid functional and standard 6-31G(d) basis set (color online).

their activity [28]. In the present work, the MEP maps of target compounds **7c**, **8b** and **8f** were investigated and the results, shown in Table 3, suggested that an electronegative area (in red) can be observed at the nitroimidazole ring, which strongly demonstrated that the long pair from nitroimidazole probably oriented toward the outer part of the molecule, thus easily interacting with various enzymes and receptors in biological systems.

3.9 Molecular docking

Molecular docking study as an effective method is widely employed in drug discovery for investigating binding modes of small molecules to biological species [29]. To rationalize the obtained antibacterial activity and elucidate the anti-*E. coli* action mechanism, molecular docking study was successfully performed between compound **8f** and *E. coli* DNA polymerase III (PDB ID: 2POL) that was of great importance for the synthesis of *E. coli* DNA. As shown in Figure 6, the nitro group of compound **8f** was in close proximity to the residue GLY-219 through hydrogen bonds with a distance of 1.6 Å and the binding energy was as low as -5.32 kJ/mol, which might be accordant with MEP effect. This interaction demonstrated that compound **8f** might disturb the synthesis of *E. coli* DNA through binding to DNA polymerase III, thus exhibiting profound antibacterial potency.

3.10 Interaction with DNA

Deoxyribonucleic acid (DNA) is of great importance for storing information to continue the life and can also be a potent drug target due to the presence of multiple sites interacting with drug molecules, which is usually exploited as an attractive approach for the rational design and construction of novel and effective drugs [30]. It has been reported that berberine and its derivatives could effectively interact with DNA through various binding modes [31]. Therefore, to explore the possible antimicrobial mechanism, the *in vitro* binding studies of highly active compound **8f** with *E. coli*

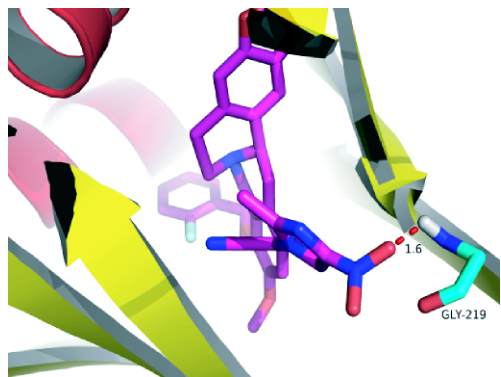


Figure 6 Molecular modeling of compound **8f** and *E. coli* DNA polymerase III (color online).

DNA, which was isolated from drug-resistant *E. coli* through a four-step process, were performed using neutral red (NR) as a spectral probe by UV-Vis spectroscopy.

The detection of hyperchromism and hypochromism by absorption spectroscopy, which are critical spectral features to distinguish the change of DNA double helical structure, is one of the most important and useful method in DNA-binding studies [32]. The observed strong hyperchromism might be attributed to the denaturation of DNA caused by the strong interaction between the electronic states of intercalating chromophore and that of the DNA base. The UV-Vis absorption spectra were recorded with gradually increasing amount of compound **8f** at a fixed concentration of DNA. As shown in Figure 7. The UV-Vis spectra revealed that the maximum absorption peak of DNA at 260 nm showed proportional increase and slight blue shift with the increasing concentration of derivative **8f**. Remarkably, the spectral information suggested that the measured absorption value of **8f**-DNA complex was a little greater than that of simply sum of free DNA and free compound **8f**. This demonstrated a constructional change in DNA duplex, which might be characteristic of non-covalent interactions between DNA and complexes resulting in some disassembly of DNA helix and the exposure of some DNA bases. In general, the observed spectral properties could be explained by the potent interaction of compound **8f** with *E. coli* DNA.

Based on the changes in the absorption spectra of DNA upon binding to **8f**, the binding constant K could be calculated by the Eq. (1), where A^0 and A represent the absorbance of DNA in the absence and presence of compound **8f** at 260 nm, ζ_C and ζ_{D-C} are the absorption coefficients of compound **8f** and **8f**-DNA complex, respectively. The plot of $A^0/(A-A^0)$ versus $1/[\text{compound } \mathbf{8f}]$ is constructed by using the

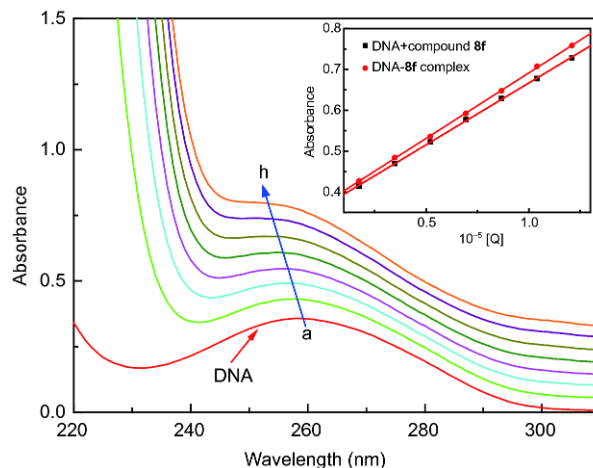


Figure 7 Interaction of resistant *E. coli* DNA with highly active molecule **8f** at different concentrations was recorded by UV absorption spectra (pH 7.4, $T=303$ K). Inset: comparison of absorption at 260 nm between the **8f**-DNA complex and the sum values of free DNA and free compound **8f**. $[\text{DNA}]=5.18\times 10^{-5}$ M, and $[\text{compound } \mathbf{8f}]=0-1.21\times 10^{-5}$ M for curves (a-h) respectively at increment of 0.174×10^{-5} M (color online).

absorption titration data and linear fitting (Figure S2, Supporting Information online), yielding the binding constant, $K=2.85\times 10^5$ L/mol, $R=0.998$, $SD=0.089$ (R is the correlation coefficient, SD is standard deviation).

$$\frac{A^0}{A-A^0} = \frac{\xi_c}{\xi_D-c-\xi_c} + \frac{\xi_c}{\xi_D-c-\xi_c} \times \frac{1}{K[Q]} \quad (1)$$

To further elucidate the interaction between compound **8f** and *E. coli* DNA, neutral red (NR, a planar phenazine dye with a confirmed intercalative binding mode with DNA) was employed as a spectral probe due to its lower toxicity and higher stability. Therefore, NR was chosen as the spectral probe to investigate the binding mode of compound **8f** with DNA in present work, and the absorption spectra of the NR dye upon the addition of DNA were shown in Figure S3. The absorption peak of NR at around 460 nm gradually decreased with the increasing concentration of DNA, and a new band at around 530 nm appeared, which could be attributed to the formation of the new DNA-NR complex [33]. The isosbestic point at 500 nm provided evidence for the formation of DNA-NR complex.

Further investigation for the mode of binding between NR and compound **8f** was carried out via the competitive interaction of NR and **8f** with DNA. As shown in Figure 8, an apparent intensity increase was observed around 460 nm along with the increasing concentration of compound **8f**. Besides, when compared with the absorption around 460 nm of free NR in the presence of the increasing concentrations of DNA (Figure S3), the absorbance at the same wavelength exhibited the reverse process (inset of Figure 8). These results strongly demonstrated that compound **8f** could effectively intercalate into the double helix of DNA by substituting NR in the DNA-NR complex.

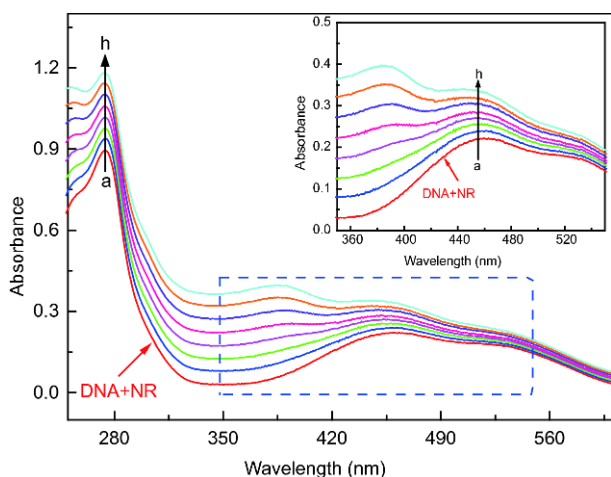


Figure 8 The competitive reaction between highly active molecule **8f** and NR with *E. coli* DNA was determined by UV absorption spectra. $[DNA]=5.18\times 10^{-5}$ M, $[NR]=2\times 10^{-5}$ M, and $[compound\ 8f]=0-1.21\times 10^{-5}$ M for curves (a-h) respectively at increment of 0.174×10^{-5} . Inset: absorption spectra of the system with the increasing concentration of **8f** in the wavelength range of 350–550 nm absorption spectra of competitive reaction between compound **8f** and NR with *E. coli* DNA (color online).

3.11 Bacterial membrane permeabilization

The exploitation of bacterial membrane active agents is an increasingly important approach to solve the problem of bacterial resistance for that the membrane-active property mostly blocks the development of resistance [34]. Therefore, the clinical drug-resistant *E. coli* was rationally chosen to investigate the ability of highly active compound **8f** to permeabilize the bacterial cell membrane using propidium iodide (PI) as dye, which could successfully pass through the membrane of compromised bacterial cells and form a complex with DNA to fluoresce. As shown in Figure 9, the fluorescence intensity of experimental group (in the presence of compound **8f**) presented stability after first experienced an upward trend with the increase in the time, while the control group almost showed no change. The observed results demonstrated that compound **8f** could effectively permeabilize the membrane of resistant *E. coli*.

3.12 Selective inhibition of bacteria

Microorganisms are able to coexist in mixed populations and can cause complex bacterial infections. Generally, in order to treat these complex infections, various types of antimicrobial drugs will be jointly used, and as a result, excess use of antibiotics accelerates the development of drug-resistance [35]. Specifically addressing a single bacterial strain from a mixture of multiple strains is a fascinating scientific challenge and a necessity in healthcare and provides an important tool in microbiology research [36]. Thus, the selectively inhibitory activity of the highly active compound **8f** with MIC value of 0.003 mM against drug-resistant *E. coli* was evaluated through incubating mixture strains (including Gram-positive bacteria *S. aureus*, Gram-negative bacteria *P. aeruginosa* and fungi *C. albicans*, respectively) on agar plate containing 0.003 mM of berberine-derived nitroimidazole **8f**. As the colony morphology was shown in Table 4, in the

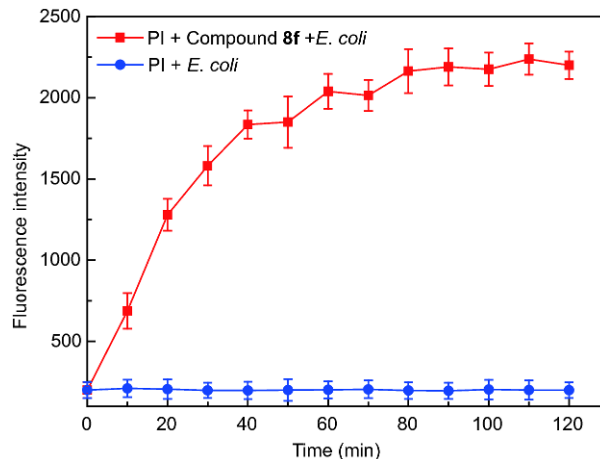
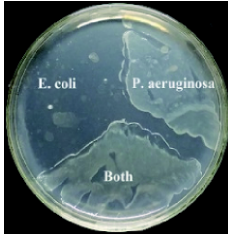
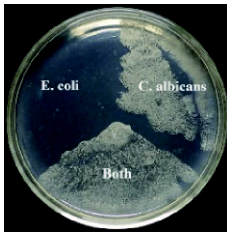
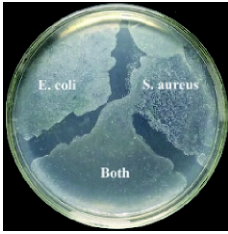
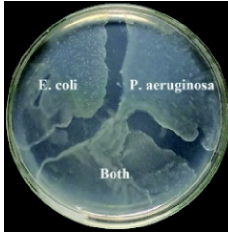
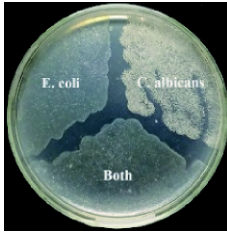


Figure 9 Membrane permeabilization of resistant bacterial *E. coli* toward compound **8f** ($12\times MIC$) (color online).

Table 4 Selectively inhibitory effect against resistant *E. coli* of highly active derivative **8f**^{a)}

	<i>E. coli</i> vs. <i>S. aureus</i>	<i>E. coli</i> vs. <i>P. aeruginosa</i>	<i>E. coli</i> vs. <i>C. albicans</i>
Presence of compound 8f			
Absence of compound 8f			

a) Representative photographs of colonies from mixed cultures incubated for 12 h in the presence and absence of 0.003 mM compound **8f**.

presence of compound **8f**, the three agar plates did not show any growth at the *E. coli* sector, while normal growth was observed at the other two sectors. Comparably, all the strains were normally growing in the absence of compound **8f**. These results demonstrated that compound **8f** exhibited the potency to selectively inhibit the growth of resistant *E. coli* from a mixture of microorganisms.

4 Conclusions

In conclusion, a series of berberine-derived nitroimidazoles were successfully developed by a convenient procedure from commercially natural berberine. Their structures were confirmed by NMR, IR and HRMS spectra. The antimicrobial evaluation *in vitro* indicated that some target molecules showed good inhibitory effects against drug-resistant bacteria (*E. coli*, *A. baumannii* and *E. faecalis*) and drug-susceptible strains (*S. aureus* ATCC25923 and *P. aeruginosa* 27853). The structure-activity relationships revealed that various substituents on 9-position of berberine skeleton

would exhibit distinct influence on the bioactivities and most of the aliphatic substituents exerted relatively potent antimicrobial property (Figure 10). However, 2-fluorobenzyl compound **8f** with an improved aqueous solubility (4.54±0.08 µg/mL) not only exerted strong activity against drug-resistant *E. coli* (MIC=0.003 mM), which was more active than berberine and norfloxacin, but also exhibited low toxicity toward RAW 264.7 cells and less propensity to trigger development of resistance. The molecular docking and quantum chemical experiments suggested that compound **8f** might target *E. coli* DNA polymerase III through the formation of hydrogen bonds. Berberine skeleton and nitroimidazole ring theoretically acted as the electron donor and receptor, respectively, to bind with various biological molecules. The further exploration of antibacterial mechanism revealed that the highly active molecule **8f** could effectively permeabilize resistant *E. coli* cell membrane and intercalate into DNA isolated from resistant *E. coli* to form **8f**-DNA complex ($K=2.85\times 10^5$ L/mol), thus blocking DNA replication. Moreover, the active molecule **8f** could selec-

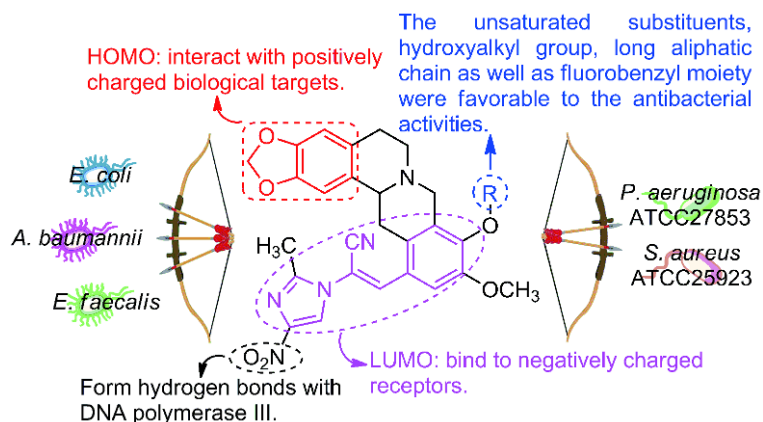


Figure 10 Preliminary summary of structure-activity relationships (color online).

tively inhibit the growth of *E. coli* from a mixture of various strains. These results strongly demonstrated that the natural berberine-derived nitroimidazole **8f** was a promising candidate as multi-targeting anti-*E. coli* drug.

Acknowledgements This work was partially supported by the National Natural Science Foundation of China (21672173, 21372186), Research Fund for International Young Scientists from International (Regional) Co-operation and Exchange Program of NSFC (81650110529), Chongqing Special Foundation for Postdoctoral Research Proposal (Xm2016039, Xm2017185), Program for Overseas Young Talents from State Administration of Foreign Experts Affairs, China (WQ2017XNDX047), the Doctoral Fund of Southwest University (SWU111075), and the Research Funds for the Central Universities (XDJK2017B015).

Conflict of interest The authors declare that they have no conflict of interest.

Supporting information The supporting information is available online at <http://chem.scichina.com> and <http://link.springer.com/journal/11426>. The supporting materials are published as submitted, without typesetting or editing. The responsibility for scientific accuracy and content remains entirely with the authors.

- Garland M, Loscher S, Bogoy M. *Chem Rev*, 2017, 117: 4422–4461
- Brown ED, Wright GD. *Nature*, 2016, 529: 336–343
- (a) Petty NK, Ben Zakour NL, Stanton-Cook M, Skippington E, Totsika M, Forde BM, Phan MD, Gomes Moriel D, Peters KM, Davies M, Rogers BA, Dougan G, Rodriguez-Baño J, Pascual A, Pitout JDD, Upton M, Paterson DL, Walsh TR, Schembri MA, Beatson SA. *Proc Natl Acad Sci USA*, 2014, 111: 5694–5699; (b) Guo Y, Liu X, Li B, Yao J, Wood TK, Wang X. *J Bacteriol*, 2017, 199: e00057
- (a) Ling LL, Schneider T, Peoples AJ, Spoering AL, Engels I, Conlon BP, Mueller A, Schäberle TF, Hughes DE, Epstein S, Jones M, Lazarides L, Steadman VA, Cohen DR, Felix CR, Fetterman KA, Millett WP, Nitti AG, Zullo AM, Chen C, Lewis K. *Nature*, 2015, 517: 455–459; (b) O'Connell KMG, Hodgkinson JT, Sore HF, Welch M, Salmon GPC, Spring DR. *Angew Chem Int Ed*, 2013, 52: 10706–10733
- (a) Peng XM, Damu GLV, Zhou CH. *Curr Pharm Des*, 2013, 19: 3884–3930; (b) Silva LN, Zimmer KR, Macedo AJ, Trentin DS. *Chem Rev*, 2016, 116: 9162–9236
- Tillhon M, Guamán Ortiz LM, Lombardi P, Scovassi AI. *Biochem Pharmacol*, 2012, 84: 1260–1267
- (a) Jeyakkumar P, Zhang L, Avula SR, Zhou CH. *Eur J Med Chem*, 2016, 122: 205–215; (b) Mistry B, Keum YS, Noorzai R, Gansukh E, Kim DH. *J Iran Chem Soc*, 2016, 13: 531–539
- (a) Endeshaw M, Zhu X, He S, Pandharkar T, Cason E, Mahasenan KV, Agarwal H, Li C, Munde M, Wilson WD, Bahar M, Doskotch RW, Kinghorn AD, Kaiser M, Brun R, Drew ME, Werbovetz KA. *J Nat Prod*, 2013, 76: 311–315; (b) Kumar A, Ekavali A, Chopra K, Mukherjee M, Pottabathini R, Dhull DK. *Eur J Pharmacol*, 2015, 761: 288–297
- Duan JR, Liu HB, Jeyakkumar P, Gopala L, Li S, Geng RX, Zhou CH. *Med Chem Commun*, 2017, 8: 907–916
- (a) Peng XM, Cai GX, Zhou CH. *Curr Top Med Chem*, 2013, 13: 1963–2010; (b) Zhang HZ, Gan LL, Wang H, Zhou CH. *Mini-Rev Med Chem*, 2017, 17: 122–166; (c) Liu HB, Gao WW, Tangadanchu VKR, Zhou CH, Geng RX. *Eur J Med Chem*, 2018, 143: 66–84
- Khalaj A, Nakhjiri M, Negahbani AS, Samadizadeh M, Firoozpour L, Rajabalian S, Samadi N, Faramarzi MA, Adibpour N, Shafiee A, Foroumadi A. *Eur J Med Chem*, 2011, 46: 65–70
- Ang CW, Jarrad AM, Cooper MA, Blaskovich MAT. *J Med Chem*, 2017, 60: 7636–7657
- Cui SF, Peng LP, Zhang HZ, Rasheed S, Vijaya Kumar K, Zhou CH. *Eur J Med Chem*, 2014, 86: 318–334
- (a) Zhang L, Peng XM, Damu GLV, Geng RX, Zhou CH. *Med Res Rev*, 2014, 34: 340–437; (b) Rouf A, Tanyeli C. *Eur J Med Chem*, 2015, 97: 911–927; (c) Zhou CH, Wang Y. *Curr Med Chem*, 2012, 19: 239–280; (d) Dai L, Cui S, Damu GLV, Zhou C. *Chin J Org Chem*, 2013, 33: 224–244
- Zhang SL, Chang JJ, Damu GLV, Fang B, Zhou XD, Geng RX, Zhou CH. *Bioorg Med Chem Lett*, 2013, 23: 1008–1012
- Wen SQ, Jeyakkumar P, Avula SR, Zhang L, Zhou CH. *Bioorg Med Chem Lett*, 2016, 26: 2768–2773
- (a) Jeyakkumar P, Liu HB, Gopala L, Cheng Y, Peng XM, Geng RX, Zhou CH. *Bioorg Med Chem Lett*, 2017, 27: 1737–1743; (b) Lai TT, Xie D, Zhou CH, Cai GX. *J Org Chem*, 2016, 81: 8806–8815
- (a) Zhang FF, Gan LL, Zhou CH. *Bioorg Med Chem Lett*, 2010, 20: 1881–1884; (b) Peng XM, Kumar KV, Damu GLV, Zhou CH. *Sci China Chem*, 2016, 59: 878–894
- (a) Su T, Xie S, Wei H, Yan J, Huang L, Li X. *Bioorg Med Chem*, 2013, 21: 5830–5840; (b) Zhang L, Chang JJ, Zhang SL, Damu GLV, Geng RX, Zhou CH. *Bioorg Med Chem*, 2013, 21: 4158–4169
- Salas PF, Herrmann C, Cawthray JF, Nimphius C, Kenkel A, Chen J, de Kock C, Smith PJ, Patrick BO, Adam MJ, Orvig C. *J Med Chem*, 2013, 56: 1596–1613
- (a) Zelikin AN, Ehrhardt C, Healy AM. *Nat Chem*, 2016, 8: 997–1007; (b) Dai LL, Zhang HZ, Nagarajan S, Rasheed S, Zhou CH. *Med Chem Commun*, 2015, 6: 147–154
- (a) von Karstedt S, Montinaro A, Walczak H. *Nat Rev Cancer*, 2017, 17: 352–366; (b) Cui SF, Addla D, Zhou CH. *J Med Chem*, 2016, 59: 4488–4510
- (a) Wolny-Koładka K, Lenart-Boroń A. *Water Air Soil Pollut*, 2016, 227: 146; (b) Hu J, Liu F, Ju H. *Angew Chem Int Ed*, 2016, 55: 6667–6670
- (a) Konai MM, Ghosh C, Yarlagadda V, Samaddar S, Haldar J. *J Med Chem*, 2014, 57: 9409–9423; (b) Gao WW, Zhou CH. *Future Med Chem*, 2017, 9: 1461–1464
- (a) Abraham CS, Prasana JC, Muthu S. *Spectrochim Acta A*, 2017, 181: 153–163; (b) Dey T, Praveena KSS, Pal S, Mukherjee AK. *J Mol Struct*, 2017, 1137: 615–625
- Cheng Y, Avula SR, Gao WW, Addla D, Tangadanchu VKR, Zhang L, Lin JM, Zhou CH. *Eur J Med Chem*, 2016, 124: 935–945
- Zhang HZ, He SC, Peng YJ, Zhang HJ, Gopala L, Tangadanchu VKR, Gan LL, Zhou CH. *Eur J Med Chem*, 2017, 136: 165–183
- Gao WW, Rasheed S, Tangadanchu VKR, Sun Y, Peng XM, Cheng Y, Zhang FX, Lin JM, Zhou CH. *Sci China Chem*, 2017, 60: 769–785
- (a) Zhang SL, Chang JJ, Damu GLV, Geng RX, Zhou CH. *Med Chem Commun*, 2013, 4: 839–846; (b) Yin BT, Yan CY, Peng XM, Zhang SL, Rasheed S, Geng RX, Zhou CH. *Eur J Med Chem*, 2014, 71: 148–159; (c) Fang XF, Li D, Tangadanchu VKR, Gopala L, Gao WW, Zhou CH. *Bioorg Med Chem Lett*, 2017, 27: 4964–4969
- (a) Shimazaki Y, Tanaka J, Kohara Y, Kamahori M, Sakamoto T. *Anal Chem*, 2017, 89: 6305–6308; (b) Addla D, Wen SQ, Gao WW, Maddili SK, Zhang L, Zhou CH. *Med Chem Commun*, 2016, 7: 1988–1994
- Jiang H, Wang X, Huang L, Luo Z, Su T, Ding K, Li X. *Bioorg Med Chem*, 2011, 19: 7228–7235
- (a) Peng LP, Nagarajan S, Rasheed S, Zhou CH. *Med Chem Commun*, 2015, 6: 222–229; (b) Zhang L, Kumar KV, Rasheed S, Zhang SL, Geng RX, Zhou CH. *Med Chem Commun*, 2015, 6: 1303–1310; (c) Li ZZ, Gopala L, Tangadanchu VKR, Gao WW, Zhou CH. *Bioorg Med Chem*, 2017, 25: 6511–6522
- Zhang Y, Damu GLV, Cui SF, Mi JL, Tangadanchu VKR, Zhou CH. *Med Chem Commun*, 2017, 8: 1631–1639
- Zhang L, Addla D, Ponmani J, Wang A, Xie D, Wang YN, Zhang SL, Geng RX, Cai GX, Li S, Zhou CH. *Eur J Med Chem*, 2016, 111: 160–182
- Velema WA, van der Berg JP, Szymanski W, Driessen AJM, Feringa BL. *ACS Chem Biol*, 2014, 9: 1969–1974
- Zheng T, Nolan EM. *J Am Chem Soc*, 2014, 136: 9677–9691